CHAPTER - VIII

INFLUENCE OF POLYESTERS ON THE CORROSION RESISTANCE OF Ti-6Al-4V ALLOY IN SIMULATED BODY FLUID

8.1 INTRODUCTION

The passion towards higher quality and secured life span has increased the demands of implant materials in medical sectors which could replenish the lost functions or replace the organs making it to function at a desirable level[1]. Selection of an implant material mainly depends on its biocompatible nature. Metallic implants can be moulded based on austenitic stainless steels, cobalt-chromium alloys (or) titanium and its alloys as reported by **Sivakumar *et al.*,**[2] along with ASTM standards. Though these materials are susceptible to body conditions, its alloying elements in trace levels can project its specific biological role. To be still precise, though cobalt-chromium alloys possess good corrosion resistance, its poor frictional properties and tedious fabrication procedures makes it unfit for joint prosthesis. Whereas austenitic stainless steels with low cost, ease fabrication, reasonable corrosion resistance, strength, fatigue resistance has made it a suitable orthopaedic implant material in India, which in the early 20th century turned out with failure due to detrimental tissue reactions[3]. Besides these two, titanium metal and its alloys credited with excellent properties like corrosion resistance[4], physical and mechanical properties[5], chemical and electrochemical stability[6] has let it to stamp in diverse applications like aerospace[7], marine, chemical industries[8] and medical fields[9] making it more significant than other alloys as stated by **Chen *et al.*,**[10] and **Hsu *et al.*,**[11].

8.1.1 Ti-6Al-4V alloys

Titanium and its alloys are the main back bone of surgical implantation whose basic structure and fabrication methods determines its property[12]. Titanium as a bare metal exists in an allotropic form which takes hexagonal close packed crystal structure (hcp) referred as alpha (α) phase at temperature ranging from 22-882^{o}C. Temperature higher than 882^{o}C, transforms hcp structure to body centred cubic (bcc) crystal structure resulting in a beta (β) phase. This transformation is facilitated by certain alloying elements like aluminium (Al), tin (Sn), vanadium (V), molybdenum (Mo), chromium (Cr), copper (Cu), zirconium (Zr) or silicon (Si) leading to α (or) β (or) α + β structures. However α + β alloy is more desirable than sole α (or) β alloy because of its stability at wide range of temperatures. As α alloys are stable at lower temperature and β alloys at higher temperature, Ti-6Al-4V alloy containing aluminium

and vanadium as α and β stabiliser behaves as α + β alloy undoubtedly being stable at higher temperatures.

Ti-6Al-4V alloy was the first registered implant material in the ASTM standards (F-136-84)[13]. Being popular, it is a deserved structural biomaterial behaving as an alternate replacement for joints, hip, knees and shoulders[14]. Such titanium alloys experience stress shielding effect after implantation within the body which may lead to its failure accompanied with detrimental resorptive bone remodelling originating due to the difference of young's modulus of titanium alloys and host bones as reported by **Busuioc *et al.,***[15]. As documented by **Mohsen *et al.,***[16] titanium implants on constant contact with aggressive body fluids containing water, dissolved oxygen, proteins, plasma, sodium and chloride ions along with electrolytes undergo corrosion reactions.

8.1.2 Review of literature

To strengthen the research based on implantation, the below review has been made based on which the present work is to be discussed.

Rikhari *et al.,* utilised dynamic electrochemical impedance spectroscopy (DEIS) technique to evaluate the corrosion resistance of Ti coated with polypyrrole (PPy) in simulated body fluid. Results obtained from impedance and polarisation technique suggested enhanced corrosion resistance of coated rather than uncoated one[17].

Sanja Erakovic *et al.,* investigated the study of silver/hydroxyapatite (Ag/HAP) and silver/hydroxyapatite/lignin (Ag/HAP/Lig) coatings on titanium alloys in simulated body fluid (SBF) rather than hydroxyapatite alone. From the studies made, it was concluded that Ag/HAP/Lig coated titanium alloy possessed good corrosion resistance[18].

Leonardo *et al.,* evaluated the corrosion resistance of Ti-6Al-4V alloy with smooth surface as well as surface modified by double acid etching in presence of various concentrations of dextrose and lipopolysaccharide in simulated body fluid. Observation of the results showed strong correlation of lipopolysaccharide with corrosion parameters for the titanium alloy treated with double acid etching[19].

Fekry *et al.,* analysed the corrosion inhibition of Ti-6Al-4V alloy in acid rain water using electrochemical techniques which showed decreased corrosion current density on increasing the pH range. Moreover addition of different anions such as Cl^-, F^- or SO_4^{2-} was also investigated which revealed increased corrosion resistance for sulphate anions[20].

Karimi *et al.,* studied the corrosion inhibition of Ti–6Al–4V in aerated buffered phosphate saline medium in presence of various concentrations of bovine serum albumin (BSA) at 37^{o}C using open circuit potential, potentiodynamic polarisation technique, linear polarisation and electrochemical impedance spectroscopy. From XPS it was concluded that the addition of BSA has enriched the passive film formed on the metal surface thereby creating lower corrosion rate[21].

Ameer *et al.,* investigated the effect of raftiline inulin in simulated body fluids for titanium alloy by varying the concentrations of inulin and immersion time. From the electrochemical impedance and potentiodynamic polarisation methods, effective inhibition was noticed for 0.25% of inulin which formed a surface layer, confirmed by scanning electron microscopy[22].

Stango *et al.,* deposited hydroxyapatite powder (HAP) electrophoretically on bare and laser treated Ti-6Al-4V alloy which was then vaccum sintered at 300^{o}C for 2 hours. Electrochemical impedance and potentiodynamic polarisation techniques adopted showed better corrosion resistance of coated samples than the bare metal which was obviously due to good adhesion on coated samples[23].

Fekry *et al.,* studied the electrochemical behaviour of Ti-6Al-4V alloy in simulated body fluid using impedance and polarisation methods. From the studies, lower corrosion current density suggested higher corrosion resistance suggesting the formation of protective film on the metal surface[24].

Mischler *et al.,* studied the fretting corrosion nature of Ti-6Al-4V alloy in contact with poly(methyl methacrylate) (PMMA) in simulated body fluid environment. From the studies, no noticeable mechanical changes were observed[25].

Narayanan *et al.,* synthesised different coatings on Ti-6Al-4V alloy using aqueous electrolytes containing calcium and phosphorous. Increased time, increased the level of coatings but coatings produced from shorter time showed better resistance in SBF medium[26].

Out of the above review, it is clearly demonstrated that the Ti-6Al-4V alloy one of the foremost important alloy in implantations has been subjected to either surface modification or coating systems in order to reduce its metal dissolution rate. Owing to its importance, the present study has been undertaken to study the influence of polyesters PGSE and MPOU

[synthesis discussed in chapter II] on titanium alloys under simulated body fluid environment (SBF) adopting electrochemical measurements under laboratory scale.

8.2 EXPERIMENTAL METHODS

8.2.1 Synthesis of polyesters

Polyesters namely poly(glycerol sebacate) polyester (PGSE) and 4-(1-(4-methoxyphenyl)cyclohexyl)phenyl 10-oxoundecanoate (MPOU) were chosen for the present discussion whose structures are predicted below.

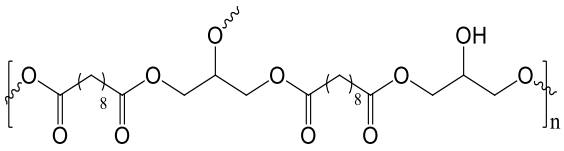

PGSE

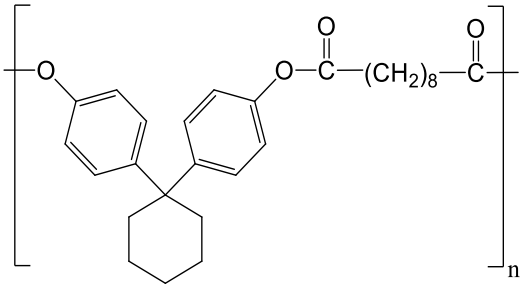

MPOU

8.2.2 Preparation of metal substrate

Titanium alloy (Ti-6Al-4V) of grade 5 was purchased from authorised dealers and machined in the required size. Prior to the study, titanium samples were polished using silicon carbide sheets followed by degreasing with acetone, dried and chemically etched using Krolls reagent (25ml H_2O+ 2 ml conc. HNO_3+ 1ml conc. HF) to remove the oxides present. Chemicals required for the preparation of simulated body fluid (SBF) as listed in the forth coming sections were purchased and used as such.

8.2.3 Preparation of simulated body fluid (SBF)

In order to simulate the human body conditions, simulated body fluid (SBF) was prepared in 1 litre of double distilled water by dissolving the reagents from 1 to 8 consecutively as listed in the **Table 1** in plastic containers placed in a water bath attached with a magnetic stirrer at 37ºC.

Reagent	Amount (g/l)
NaCl	8.035
$NaHCO_3$	0.355
KCl	0.225

$K_2HPO_4.3H_2O$	0.231
$MgCl_2.6H_2O$	0.311
$CaCl_2$	0.292
Na_2SO_4	0.072
$(OHCH_2)_3CNH_2$	6.118
1M HCl	40 ml

Table 1 Preparation of SBF

After ensuring complete dissolution of all the reagents, 1 M HCl was added to adjust the pH around 7.4. SBF prepared as documented by **Kokubo *et al.*,**[27] was then transferred to a container and stored for further usage.

8.2.4 Electrochemical measurements

Electrochemical measurements were carried out in a three electrode network comprising of platinum and calomel electrode as counter and reference electrode whereas Ti-6Al-4V alloy with an exposure area of 1 cm^2 was taken as working electrode. Simulated body fluid (SBF) of 100 ml volume was considered as physiological medium of the present discussion. Using the instrumental set up of AUTOLAB, assisted with Nova software the present study was made after attaining a steady state open circuit potential (OCP). Impedance study was made within a frequency range of 100 MHz – 100 KHz at an amplitude of 10 mV/sec followed by varying the potential from ±1500 mV at a scan rate of 1 mV/sec to record potentiodynamic polarisation curves.

8.2.5 Surface morphology – Scanning electron microscopy (SEM) and energy dispersive x-ray spectroscopy (EDS)

To confirm the adsorption of polyesters on the Ti-6Al-4V alloy, the titanium specimen was immersed in simulated body fluid (SBF) for about 6 hours with and without optimised concentration of polyester additives. The samples retrieved were subjected to scanning electron microscopy analysis (SEM) using ziess analyser followed by predicting its elemental composition by recording energy dispersive X-ray spectroscopy (EDS).

8.3 RESULTS AND DISCUSSION

8.3.1 Electrochemical impedance spectroscopy (EIS)

Electrochemical impedance spectroscopy is a most important technique to analyse the systems under investigation[28]. EIS measurements recorded for Ti-6Al-4V alloy immersed in SBF in the absence and presence of inhibitors PGSE and MPOU are displayed in **Figs. 8.1-8.2**. Nyquist plots recorded for the concentrations of 10, 100, 1000 ppm showed a straight line at 45^o which obviously indicated diffusion controlled process[29]. From the figures it is clear that the increase in diffused pattern on increasing the concentration of the inhibitors PGSE and MPOU is an indication of the formation of duplex dense layer comprising of external porous and internal compact layer where the compact layer predominantly acts as a barrier against the ion dissolution. On simulating the obtained data with the equivalent circuit shown below in **Fig. 1**, various impedance data were elicited and presented in **Table 8.1**.

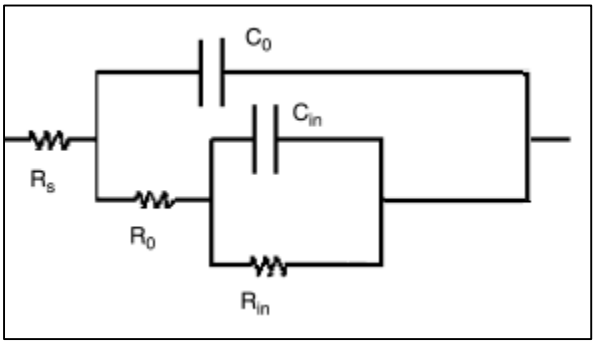

Fig. 1 Equivalent circuit to simulate EIS data

where R_s is the solution resistance, R_o and C_o are the outer porous layer resistance and capacitance, R_{in} and C_{in} are inner compact layer resistance and capacitance.

On examining the data represented in **Table 8.1**, higher resistance values for inner compact layer (R_{in}) than the outer porous layer (R_o) favoured reduced corrosion rate due to the inner layer of passive TiO_2[30]. The Ti-6Al-4V alloy possess TiO_2, TiO and Ti_2O_3 in inner metal oxide interface and oxide solution interface enriched with Al_2O_3 and V_2O_3 or V_2O_5[31] which is thermodynamically unstable. It is generally stated that vanadium oxide formed on the surface of Ti-6Al-4V alloys gradually dissolve which is further enhanced by the chloride ions of electrolyte[32]. This dissolution generates diffusion of vacancies in inner oxide layer of titanium alloy which could get dissolved in water as represented below,

$$\{TiO_2\}_s + 2H_2O \longleftrightarrow Ti(OH)_{4\,(aq)}$$

It is noticed that the passive layer formed on the metal surface is no longer stable which could readily undergo metal release in physiological medium. The passive layer on regeneration, calcium and phosphate ions of SBF medium can interrupt as shown in the below equations to form calcium phosphate layer[33].

$$\{Ti\text{-}OH\}_{solid} + Ca^{2+}_{(aq)} \longleftrightarrow \{TiO^{-} \text{ ---- } Ca^{2+}_{(aq)}\}_{solid} + H^{+}_{(aq)}$$

$$\{Ti\text{-}OH\}solid + H_2PO_4^{-}{}_{(aq)} \longleftrightarrow \{Ti\text{------ } H_2PO_4^{-}{}_{(aq)}\} + OH^{-}_{(aq)}$$

$$3Ca^{2+}_{(aq)} + 2PO_4^{3-}{}_{(aq)} \longleftrightarrow Ca_3(PO_4)_{2solid}$$

Under this circumstance, the added inhibitors could synergistically react with the adsorption of calcium and phosphate ions by getting adsorbed on the voids of the inner layer to prevent further metal dissolution. In addition increased value of solution resistance (R_s) of inhibited medium compared to blank (14.16 Ω cm^2) shows that the added inhibitors has minimised the leaching of metal ions into the test medium. Moreover decreased value of capacitance of inner compact layer from 9.84 μF/cm^2 (blank) suggested the minimised intrusion of aggressive ions towards the metal surface thereby retarding the metal dissolution.

8.3.2 Potentiodynamic polarisation studies

Figs. 8.3-8.4, shows the potentiodynamic polarisation curves of Ti-6Al-4V alloys immersed in SBF medium in the absence and presence of inhibitors PGSE and MPOU. Observing the Tafel curves of uninhibited and inhibited medium, an active –passive behaviour is noticed suggesting the occurrence of electrochemical reaction. From the polarisation curves, various parameters like corrosion current density (I_{corr}), corrosion potential (E_{corr}) and Tafel slopes (b_a and b_c) were drawn and listed in **Table 8.2**. Since the observed Tafel curves are nonlinear, Tafel constants were calculated from the slopes of immediate points after E_{corr} values. On observing both the figures, it is evident that the added additives has shifted the corrosion potential to more negative region[34] in turn reducing the corrosion current from 2.05 $x10^{-1}$ μA/cm^2 (Blank) that could be correlated with **Table 8.2**. Thus it is assumed that the added polymers behave as interface inhibitor capable of adsorbing and interacting with the metal alloy surface by means of its functional groups as reported for albumin[35] thereby reducing the effective surface area prone to corrosion[36]. However it is generally assumed that the titanium alloys in SBF medium would undergo the following typical reactions.

- The existence of Ti^{4+} at the interface between titanium and titanium dioxide as a result of the following reaction could create excess metal ions and electrons inside the

oxide. These excess charges are capable of moving within the lattices of metal to get diffused towards outside the oxide.

$$Ti \Longleftrightarrow Ti^{4+} + 4e^{-}$$

- When such Ti^{4+} comes in contact between the interface of the oxide film and SBF, chloride ions of SBF combines with the ions to form soluble alkali chloride which again enters into the SBF solution. This is because of strong oxidising capacity of chloride which makes it preferentially adsorbed on the passivation film[37].

$$Ti^{4+}_{ox} + Cl^{-}_{aq} + H_2O \longrightarrow [Ti.Cl.OH]^{2+}_{ox} + H^{+}_{aq}$$

$$[Ti.Cl.OH]^{2+}_{ox} \longrightarrow [Ti.Cl.OH]^{2+}_{aq}$$

$$[Ti.Cl.OH]^{2+}_{aq} + 2H_2O = [Ti(OH)_3]Cl + 2H^{+}_{aq}$$

Based on the above reactions it could be suggested that the added inhibitors could act synergistically by getting adsorbed on the metal surface by its lone pair electrons of oxygen atom (PGSE) and with aromatic pi electrons of MPOU inhibitor. This has the capability of covering the surface to a larger extent so that the diffusion of Ti^{4+} into SBF medium gets retarded thereby minimising the consecutive steps as shown above, in turn reducing the dissolution of titanium alloy in SBF medium.

This proposed reason also coincides well with the experimental values obtained where the decreased solution resistance (R_s), increased inner compact layer resistance (R_{in}) as well as decreased corrosion current density (I_{corr}) obtained for MPOU around 20.46 Ω cm^2, 10.585 KΩ cm^2, 3.75x10^{-3} μA/cm^2 suggested it as a better inhibitor than PGSE in SBF medium.

8.3.3 Surface morphology – Scanning electron microscopy (SEM) and energy dispersive x-ray spectroscopy (EDS)

Fig. 8.5 and **Fig. 8.6** represents the SEM and EDS images of titanium alloy immersed in simulated body fluid medium in the absence and presence of polyesters (PGSE and MPOU. From the image shown in **Fig. 8.5(a)**, it can be revealed that titanium alloy in the absence of inhibitor has undergone mild dissolution initiating localised corrosion displayed in the form of rough appearance. This is evident from its EDS spectra shown in **Fig. 8.6(a)**. On the other hand, **Fig. 8.5(b,c)** shows the adsorption of the added polyesters on the titanium alloy surface thereby forming a surface layer retarding localised corrosion and preventing the contact between the metal and electrolyte. It could be additionally evidenced from the elemental composition displayed in the **Table 8.3** and the EDS spectra **(Fig. 8.6 (b,c))** where the

additional peaks corresponding to carbon and oxygen confirms the adsorption of the added polyesters on the titanium alloy surface. Moreover the percentage of carbon and oxygen displayed in **Table 8.3** concludes the adsorption of polyesters on the titanium alloy surface.

8.4 CONCLUSIONS

(i) PGSE and MPOU were tested for its inhibition efficiency under simulated body fluid medium.

(ii) Impedance measurements carried out showed the priority of corrosion resistance by inner compact layer (R_{in})

(iii) Decreased I_{corr} values suggested the retardation of titanium alloy dissolution.

(iv) From the measurements carried out, MPOU was found to be a better inhibitor than PGSE

8.5 REFERENCES

1. S. Luiz de Assis, S.Wolynec, I. Costa, Electrochim. Acta., 51 (2006) *1815*–1819.
2. M. Sivakumar, S. Rajeswari, J. Mater. Sci. Lett., 11(15) (1992) 1039–1042.
3. R.M. Pilliar, G.C. Weatherly, Crit. Rev. Biocompatibility, 1 (1984) 371-403.
4. K. Niespodziana, K. Jurczyk, M. Jurczyk, Rev. Adv. Mater. Sci., 18 (2008) 236–240.
5. Cvijovic-Alagic, Z. Cvijovic, S. Mitrovic, V. Panic, M. Rakin, Corros. Sci., 53(2) (2011) 796–808.
6. M. Geetha, A.K. Singh, R. Asokami, A.K. Gogia, Prog. Mater. Sci., 54(3) (2009) 397–425.
7. M.F. Lopez, A. Gutierre, J. Jimenez, Electrochim. Acta., 47(9) (2002) 1359−1364.
8. N. A. Al-Mobarak , A. A. Al-Swayih, F. A. Al-Rashoud, Int. J. Electrochem. Sci., 6 (2011) 2031 – 2042.
9. R.M. Abou Shahba, W.A. Ghannem, A. El-Sayed El-Shenawy, A.S.I. Ahmed, S.M. Tantawy, Int. J. Electrochem. Sci., 6 (2011) 5499 – 5509.
10. Y. Chen, J.C. Lin, C. Ju, Mater. Des., 54 (2014) 515-519.
11. H. Hsu, S. Wu, S. Hsu, C. Li, W. Ho, Mater. Des., 65 (2015) 700-706.
12. G. S. Brady, H. R. Clauser, Materials Handbook, New York: McGraw-Hill, (1991) 13th edition.
13. T. Akahori, M. Niinomi, Mater. Sci. Eng. A., A(243) (1998) 243-237.
14. M. Huber, G. Reinisch, G. Trettenhahn, Acta Biomat., 5(1) (2009) 172–180.
15. C. Busuioc, G. Voicu, I.D. Zuzu, D. Mlu, C. Sima, F. Iordache, S.I. Jinga, Ceram. Int., 43(7) (2017) 5498-5504.
16. E. Mohsen, E. Zalnezhad, A.R. Bushroa, A.M. Hamouda, B.T. Goh, G.H. Yoon, Ceram. Int., 41(10) (2015) 14447-14457.
17. B. Rikhari, S.P. Mani, N. Rajendran, 6 (2016) 80275-80285.
18. S. Erakovic, A. Jankovic, D. Veljovic, E. Palcevskis, M. Mitric, T. Stevanovic, D. Janackovic, V. Miskovicc-Stankovic, J. Phys. Chem. B., 117(6) (2013) 1633−1643.
19. P.F. Leonardo, G.A. Wirley, P. Carvalho, J. Chia-Chun Yuan, C. Sukotjo, M.T. Mathew, V.A. Barao, PLos One., 9(3) (2014) 10.1371 /journal .pone. 0093377.
20. M.A. Fekry, R.H. Tammam, Ind. Eng. Chem. Res., 53(8) (2014) 2911−2916.
21. S. Karimi, T. Nickchi, A. Alfantazi, Corros. Sci., 53(10) (2011) 3262–3272.
22. M. A. Ameer, A. A. Ghoneim, A. M. Fekry, Surf. Interface Anal., 46(2) (2014) 65–71.
23. S.A.X. Stango, D. Karthick, S. Swaroop, U.K. Mudali, U. Vijayalakshmi, Ceram. Int., 44(3) (2018) 3149-3160.

24. A.M. Fekry, R.M. El-Sherif, Electrochim. Acta., 54(28) (2009) 7280–7285
25. S. Mischler, S. Barril, D. Landolt, Tribology – Mater. Surf. Interface., 3(1) (2009) 16-23.
26. R. Narayanan, P. Mukherjee, S. K. Seshadri, Int. J. Surf. Eng. Coat., 84(3) (2006) 134-140.
27. T. Kokubo, H. Takadama, Biomaterials, 27 (2006) 2907-2915.
28. W. G. Proud, C. Muller, Electrochim. Acta., 38(2-3) (1993) 405–413.
29. M.J. Garcia-Ramirez, R. Lopez-Sesenes, I. Rosales-Cadena, J.G. Gonzalez-Rodriguez, J. Mater. Res. Technol., (2017) https://doi.org/10.1016/j.jmrt.2017.07.003.
30. I. Milosev, T. Kosec, H.H. Strehblow, Electrochim Acta., 53(9) (2008) 3547–3558.
31. M. E. P. Souza, L. Lima, C. R. P. Lima, C. A. C. Zavaglia, C. M. A. Freire, J. Mater. Sci. Mater. Med., 20(2) (2009) 549–552.
32. M. Metikos-Hukovic, A. Kwokal, J. Piljac, Biomaterials., 24(21) (2003) 3765–3775.
33. G. Manivasagam, D. Dhinasekaran, A. Rajamanickam, Recent. Pat. Corros. Sci., 2 (2010) 40-54.
34. X.L. Cheng, S.G. Roscoe, Biomaterials, 26(35) (2005) 7350-7356.
35. L. Burgos-Asperilla, M.C. Garcia-Alonso, M.L. Escudero, C. Alonso, Acta Biomaterialia, 6(2) (2010) 652-661.
36. F. Contu, B. Elsener and H. Böhni, Corros. Sci., 46(9) (2004) 2241-2254.
37. X. Zhang, S. Yu, Z. He, Y. Liu, Corros. Sci. Prot. Technol., 15 (2003) 249–253.

Table 8.1 AC-impedance parameters for the corrosion of Ti-6Al-4V alloy for selected concentrations of the polyesters in SBF

Name of the inhibitor	Conc. (ppm)	R_s (Ω cm^2)	R_o (KΩ cm^2)	C_o (μF/ cm^2)	n_o	R_{in} (KΩ cm^2)	C_{in} (μF/ cm^2)	n_{in}
BLANK	-	14.16	4.063	10.17	0.821	4.842	9.84	0.845
PGSE	10	15.55	4.354	9.63	0.749	6.721	8.71	0.736
	100	16.71	7.813	8.94	0.852	9.249	7.99	0.850
	1000	18.43	8.438	6.79	0.829	10.134	5.32	0.933
MPOU	10	17.24	6.745	8.34	0.918	8.924	8.03	0.967
	100	18.23	9.782	7.26	0.954	10.195	6.39	0.950
	1000	20.46	9.448	5.38	0.929	10.585	4.15	0.942

Table 8.2 Potentiodynamic polarisation parameters for the corrosion of Ti-6Al-4V alloy for selected concentrations of the polyesters in SBF

Name of the inhibitor	Conc. (ppm)	Tafel slopes (mV/dec)		-Ecorr (mV)	I_{corr} ($\mu A/cm^2$)
		b_a	b_c		
BLANK	-	48	130	590.2	2.05×10^{-1}
PGSE	10	19	127	597.8	2.54×10^{-2}
	100	24	131	627.3	2.39×10^{-2}
	1000	27	163	717	1.25×10^{-2}
MPOU	10	81	176	580.6	8.97×10^{-3}
	100	105	142	620.8	6.12×10^{-3}
	1000	170	155	657.2	3.75×10^{-3}

Table 8.3 Elemental composition

Element (At %)	Ti-6Al-4V alloy	PGSE inhibited	MPOU inhibited
Ti	66.79	5.02	16.51
V	1.95	0.12	0.32
Al	22.75	1.68	2.28

Si	8.51	0.42	0.74
P	-	0.03	1.1
Mg	-	0.7	-
Ca	-	0.08	1.07
C	-	49.11	49.23
O	-	42.84	27.98
S	-	-	0.77

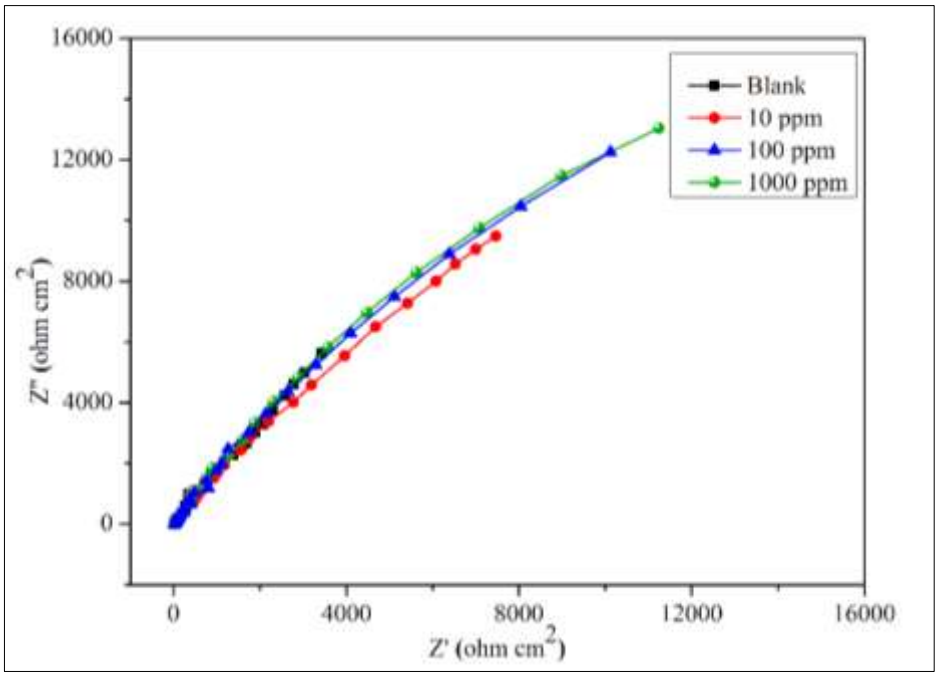

Fig. 8.1 Nyquist plots for Ti-6Al-4V alloy in SBF in the presence and absence of PGSE

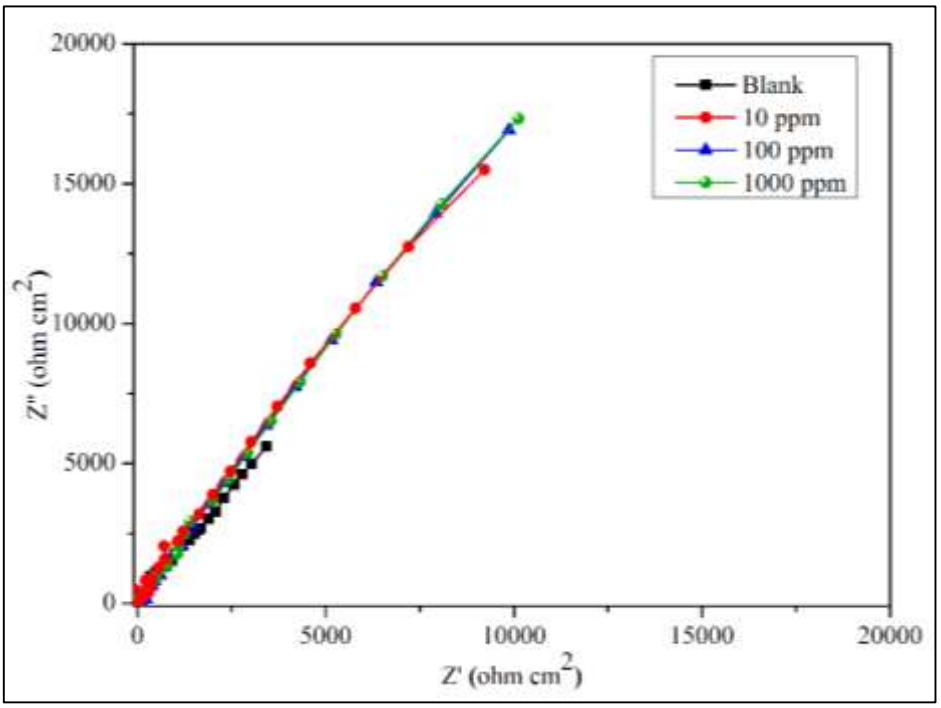

Fig. 8.2 Nyquist plots for Ti-6Al-4V alloy in SBF in the presence and absence of MPOU

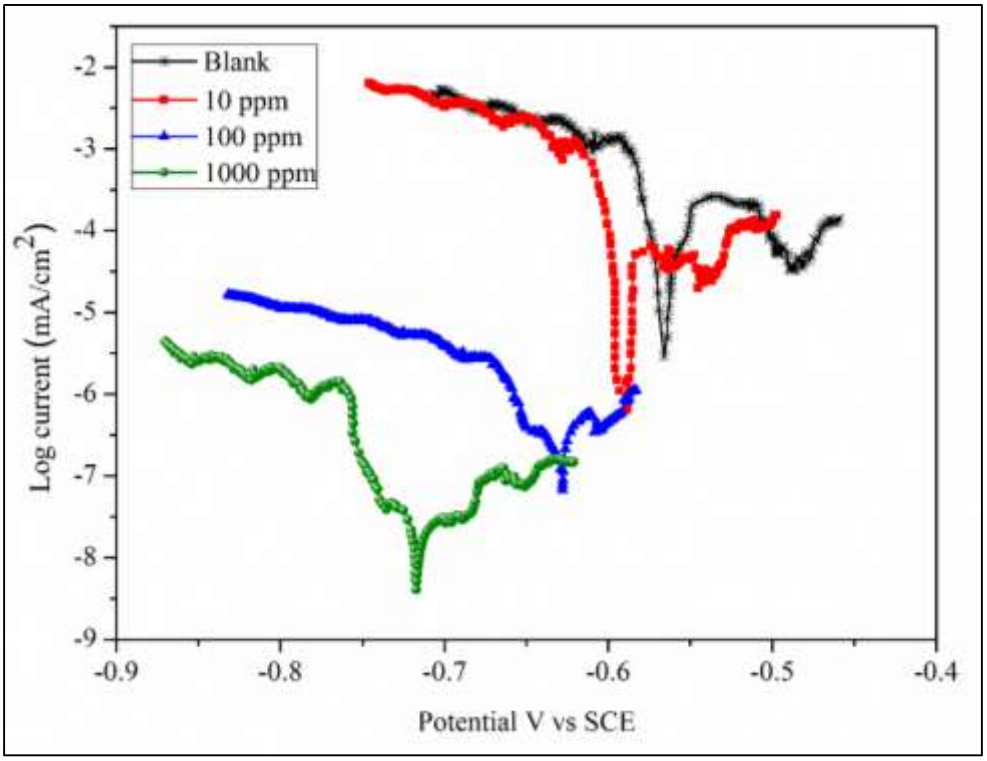

Fig. 8.3 Potentiodynamic polarisation plots for Ti-6Al-4V alloy in SBF in the presence and absence of PGSE

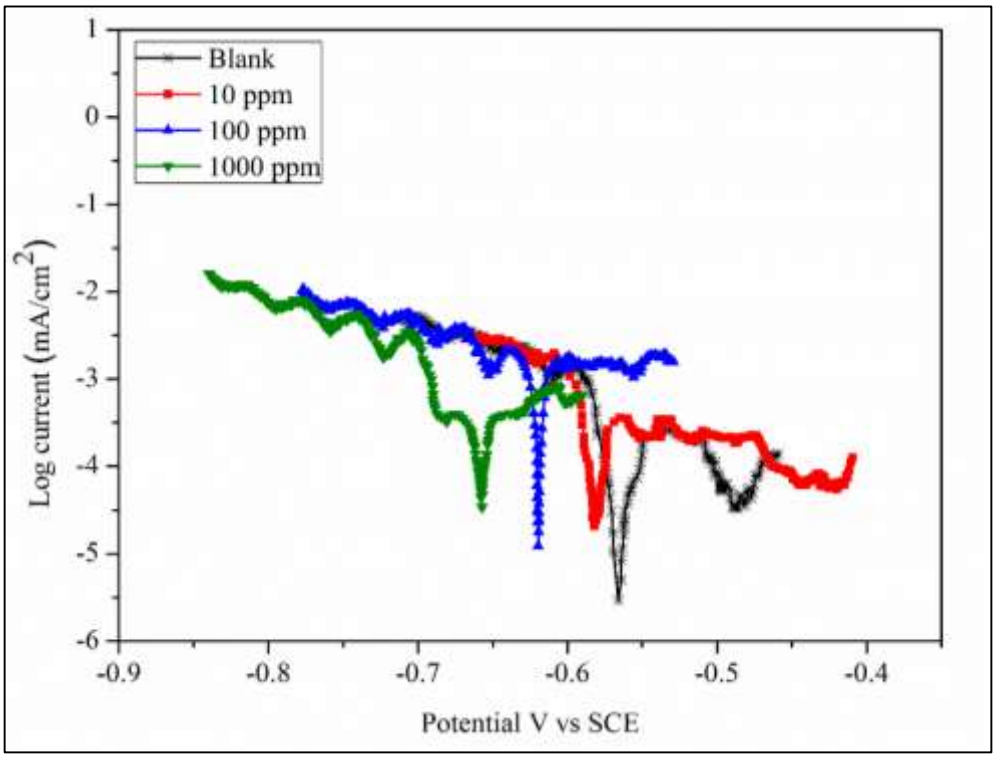

Fig. 8.4 Potentiodynamic polarisation plots for Ti-6Al-4V alloy in SBF in the presence and absence of MPOU

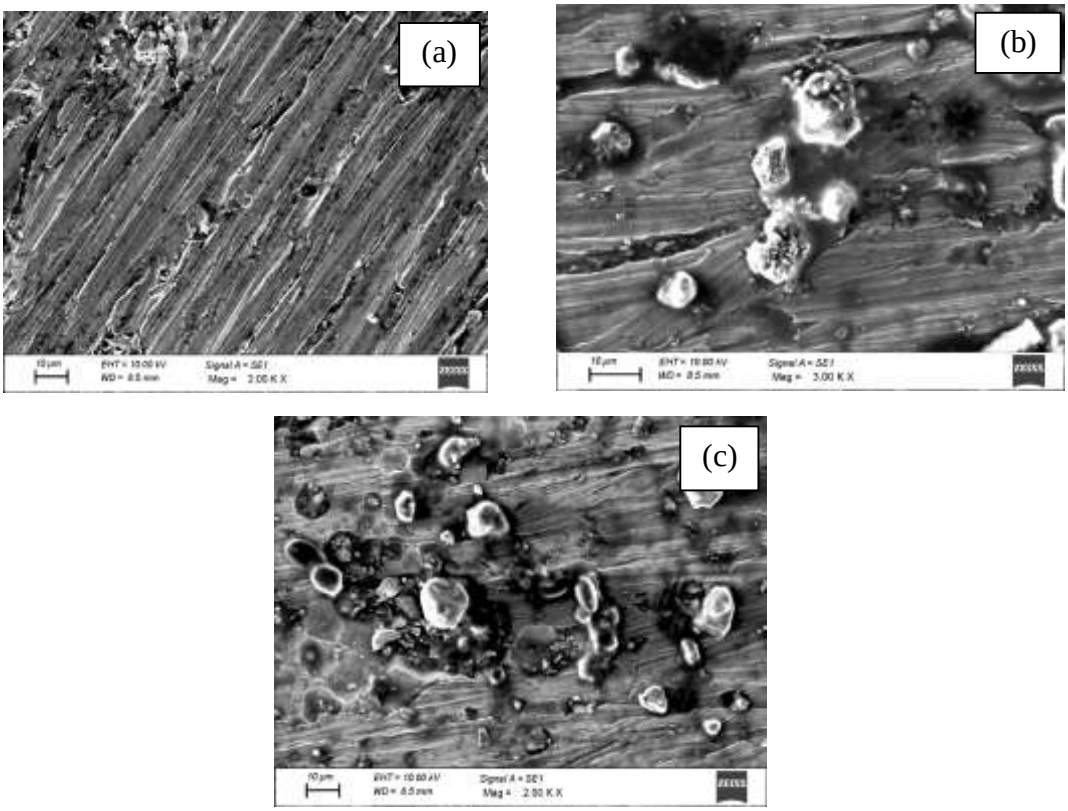

Fig. 8.5 Scanning electron microscope images of a) Ti-6Al-4V alloy b) PGSE inhibited alloy c) MPOU inhibited alloy

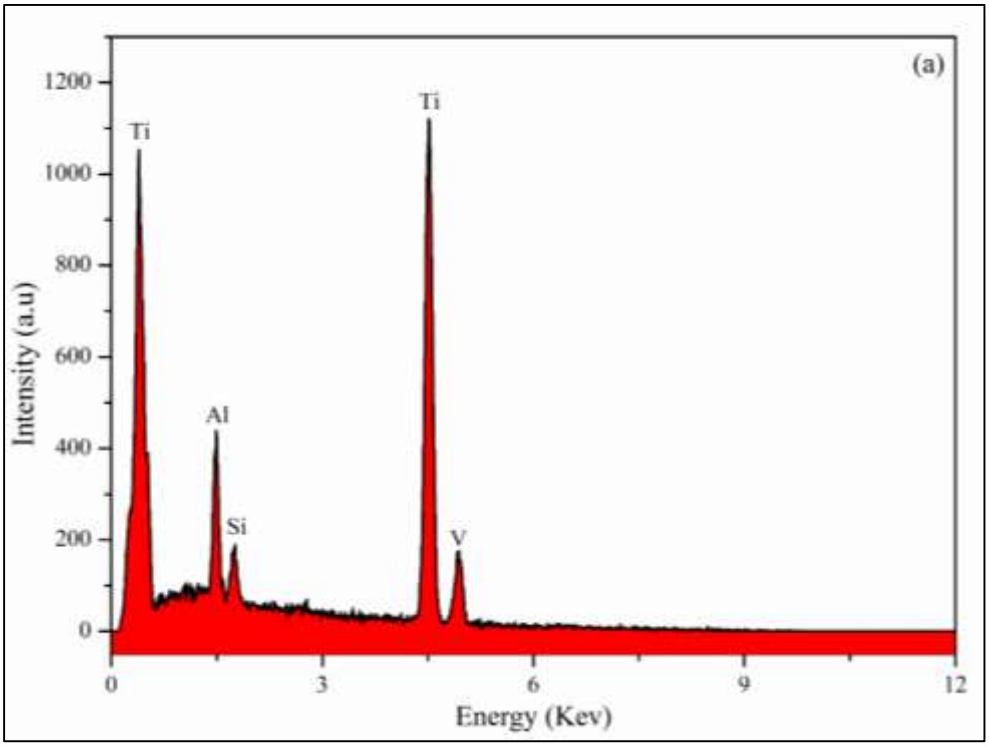
(a)
Ti
Ti
Al
Si
V
Intensity (a.u)
Energy (Kev)
0
200
400
600
800
1000
1200
0
3
6
9
12

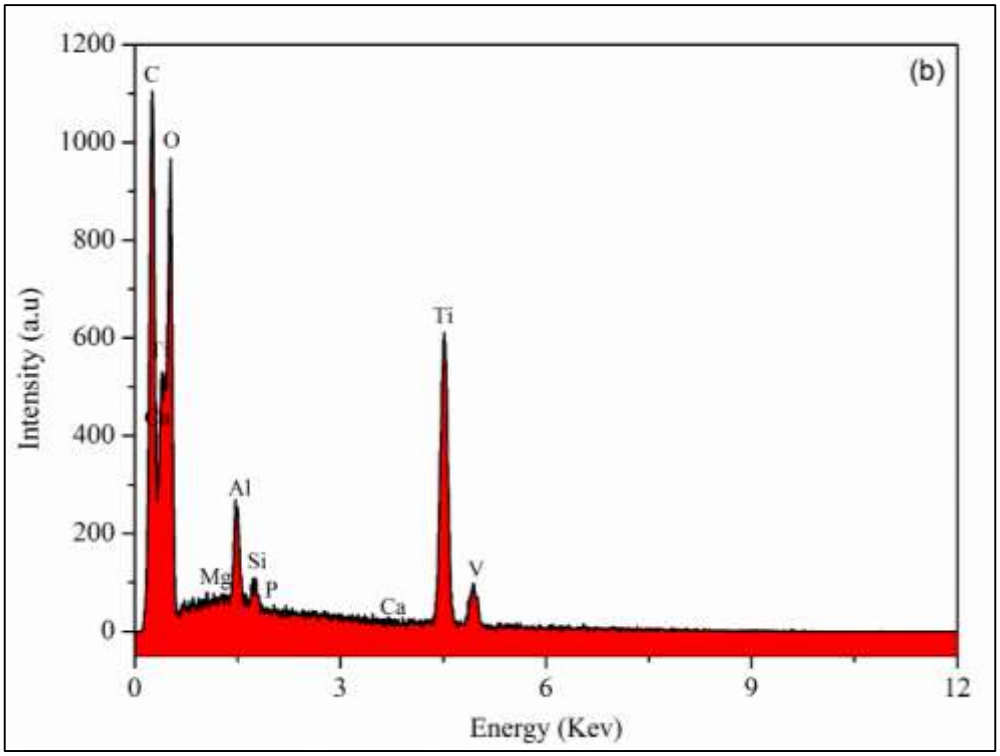
(b)
C
O
Ti
Al
Mg
Si
P
Ca
V
Intensity (a.u)
Energy (Kev)
0
200
400
600
800
1000
1200
0
3
6
9
12

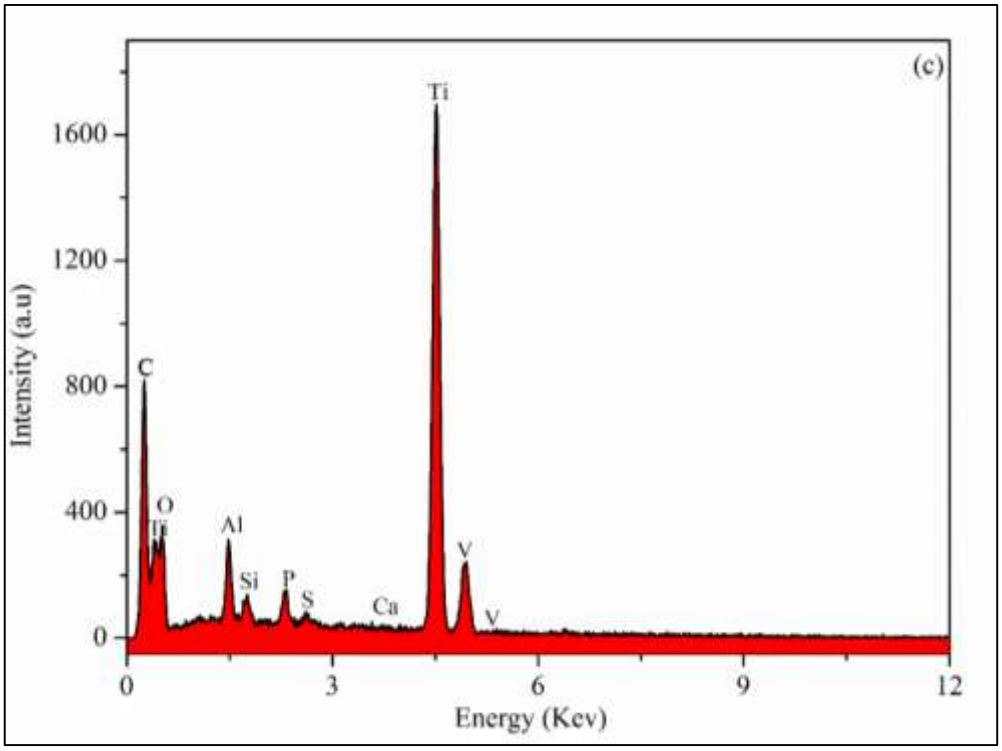

Fig. 8.6 Energy dispersive spectroscopy images of a) Ti-6Al-4V alloy b) PGSE inhibited alloy c) MPOU inhibited alloy